小児科診療〔第69巻・第11号〕別刷

2006年11月1日発行

発行所 株式会社 診断と治療社

Ⅲ．診断の進歩

病理診断法の進歩

渡部 和彦（わたべ かずひこ）
（財）東京都医学研究機構東京都神経科学総合研究所
神経細胞機能研究分野分子神経病理研究部門

要旨

先天代謝異常症のうち，とくにライソゾーム病を中心とする蓄積症には，脳神経系を侵すものが多く，神経細胞内の封入体蓄積を主体とするその病理組織学的所見は非常に多彩である．本稿では，ライソゾーム病のうち，おもなスフィンゴリピドーシスの神経病理について概説し，ライソゾーム病モデルマウスを用いた研究についてもふれる．

Key Words
神経病理
ライソゾーム病
スフィンゴリピドーシス
疾患モデルマウス

はじめに

先天代謝異常症のうち，とくにライソゾーム病を中心とする蓄積症には，脳神経系を侵すものが多いが，近年の酵素補充療法によっても，神経症状の改善に関しては多くを望めず，蓄積症における神経系異常の病態を解明し，新たな治療法を開発することが重要である．

本稿では，ライソゾーム病のうち，おもなスフィンゴリピドーシスの神経病理について概説し，ライソゾーム病モデルマウスを用いた研究についてもふれる．神経病理学は，ヒト疾患への形態学的アプローチを基本とするが，先天代謝異常症のような比較的稀少な疾患に関しては，剖検例が少なく十分な検索がなされているとは言い難い．むしろ，ヒトと同じ遺伝子変異を有する疾患遺伝子変異マウスの病理組織を詳しく解析・検索することにより，当該ヒト疾患の病理の本質に迫り，またモデルマウスを用いた治療実験を通して，治療法に関する大きな成果を生むことが期待されている．

GM1ガングリオシドーシス

Acid β-galactosidaseの欠損によりGM1 ganglioside が肝臓，脾臓，中枢神経系に蓄積する．もっとも予後不良な幼児型では肝脾腫を呈し，

0386-9806/06/¥100/頁/JCLS

肝臓，脾臓，リンパ節，骨髄にPAS陽性の泡沫細胞が多数出現する．脳はびまん性に萎縮し，大脳，脳幹，小脳，脊髄，末梢神経節のすべての神経細胞は膨化し，PAS陽性物質が充満しており，電顕的に層状の膜様封入体（membranous cytoplasmic bodies；MCBs）がみられる．Acid β-galactosidase遺伝子ノックアウトマウスの神経病理所見はヒトと同様である[1]．

GM2ガングリオシドーシス

β-hexosaminidaseの欠損によるもので，Tay-Sachs病では*HEXA*遺伝子異常によりα-subunitが欠損しHexA, HexSアイソザイムが作られなくなり，Sandhoff病では，*HEXB*遺伝子異常によりβ-subunitが欠損しHexBアイソザイムが作られなくなる．このほか，GM2 ganglioside の分解に必要なGM2 activatorの遺伝子異常でも同様の臨床症状を呈する．Tay-Sachs病およびGM2 activator異常では，病変は基本的に神経系に限られる．Tay-Sachs病では，脳は中程度に萎縮するが，2歳以降経過した例では脳重は増大することがある（megalencephaly）．すべての神経細胞は膨化しPAS陽性物質が充満し，大脳皮質錐体細胞層にmeganeuritesを認め，小脳プルキンエ細胞の脱落が著明である．

電顕的には細胞質にMCBsが蓄積し，そのおもな構成成分はGM2 ganglioside,コレステロール，リン脂質と考えられている．

一方，Sandhoff病では神経系のほかに，肝，膵，脾の細胞にPAS陽性の蓄積物質を認める．Sandhoff病の神経系にもTay-Sachs病と同様のMCBsを認めるが，ceramide trihexoside（CTH）の含量が多く，縦縞状のzebra bodiesなどさまざまな形態を呈するものが神経細胞のほかグリア細胞にも認められる．*HEXB*遺伝子ノックアウトマウスはヒトSandhoff病と同様の表現型を示す（図-A～C）[2)~4)]．

Niemann-Pick病A, B型

Acid sphingomyelinase欠損によりsphingomyelinが蓄積する疾患で，A型は神経系病変と肝脾腫を呈し急性に進行し，B型は内臓病変のみで神経病変を欠き，経過も緩徐である．A型では脳全体の強い萎縮がみられ，中枢神経系，末梢神経節の神経細胞は膨化しMCBsで充満しており，MCBsを容れたマクロファージも多数認められる．Acid sphingomyelinase遺伝子ノックアウトマウスもA型と同じ病理像を呈する[5]．

Niemann-Pick病C型

Niemann-Pick病A, B型と異なり，C型（NPC）は細胞内コレステロール輸送障害に起因する疾患であり，その95％以上はNPC1蛋白の異常，残りはNPC2蛋白の異常であることがわかっているが，NPC1, NPC2蛋白ともにその生理的な役割はまだ十分には解明されていない．本疾患でも脳の萎縮と肝脾腫がみられ，内臓器にはPAS陽性の泡沫細胞（マクロファージ）を認め，組織像はNiemann-Pick病A, B型と非常に類似している．神経系では小脳プルキンエ細胞の変性脱落が特徴的であるが，中枢・末梢神経系全域にわたって神経細胞内にMCBsが蓄積し，抗生物質filipinを用いた組織切片上の非エステル化コレステロールUV蛍光検出により確定診断が可能である．

また，コレステロールのほかにGM2, GM3 gangliosideが神経細胞内に蓄積することが見出されているが，そのメカニズムはなお不明である．特筆すべき点として，NPC脳に多数のAlzheimer神経原線維変化（neurofibrillary tangle：paired herical filaments）が出現することが以前から知られており，加えてリン酸化α-synucleinも見出されたことから，コレステロール代謝とAlzheimer病発症メカニズム解明のための

ひとつのモデルとして研究がすすめられている[6]．一方，NPCモデルマウスとしては，spmマウス，BALB/c^{nihnpc}マウスがあり（図-D～F）[7,8]，遺伝子解析，病態解明に重要なモデルとなっているが，残念ながら，これらマウスには神経原線維変化は認められない．

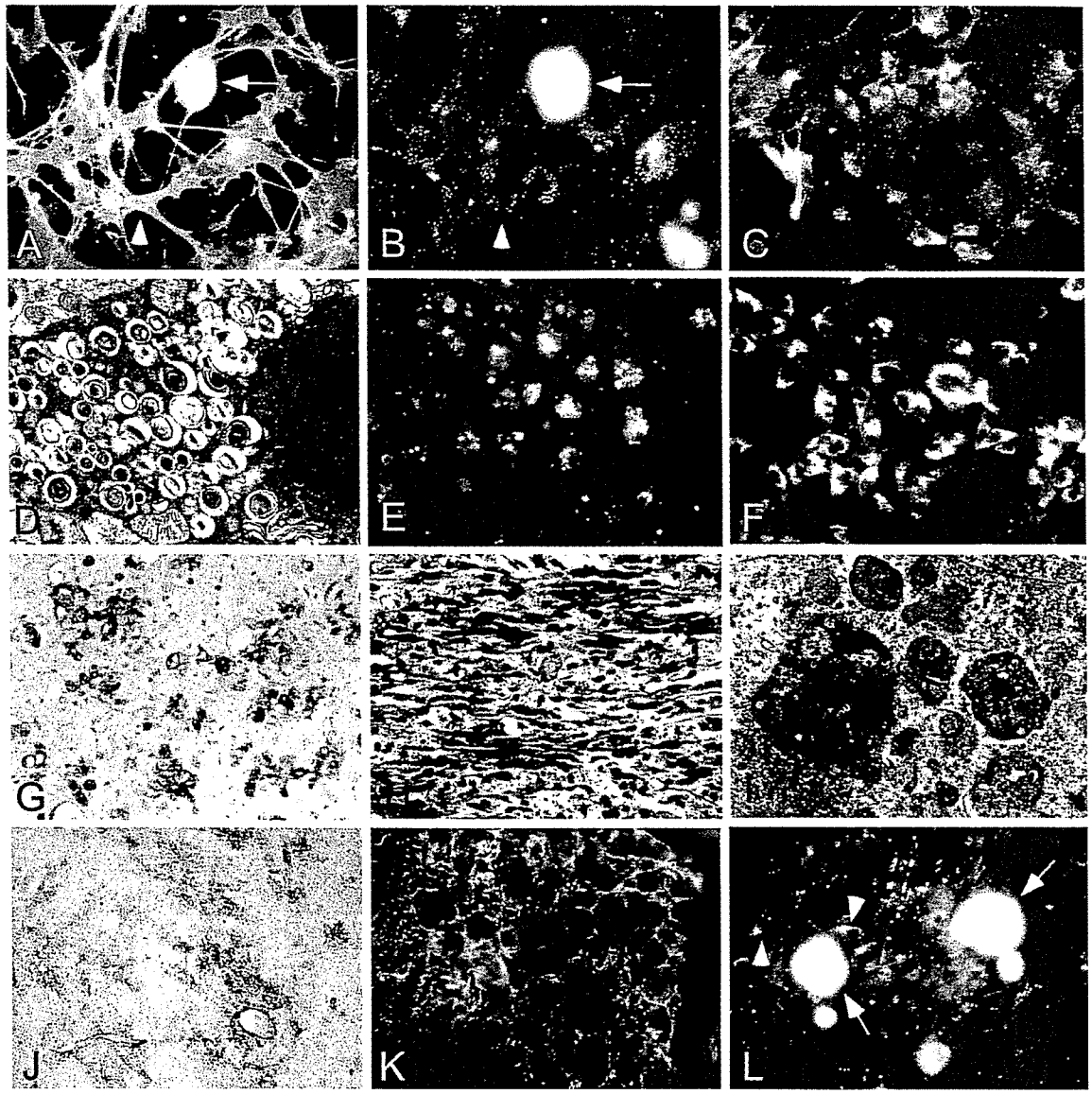

図

A～C：Sandhoff病モデルマウス後根神経節の培養．初代培養ではp75蛍光免疫染色（A）陽性のニューロン（←），シュワン細胞（◀）がGM2蛍光免疫染色（B）で陽性．（C）は長期培養により樹立した不死化シュワン細胞株のGM2蛍光免疫染色

D～E：Niemann-Pick病C型モデルマウス．D：spmマウス大脳皮質神経細胞内にみられるmembranous cytoplasmic bodies（MCBs）の電顕像．E：spmマウス視床のfilipin染色に染まるマクロファージ．F：BALB/c^{nihnpc}マウス後根神経節の長期培養により樹立した不死化シュワン細胞株のfilipin染色像

G～H：Twitcherマウス．G：脳幹部に集簇するIB4レクチン陽性マクロファージ．H：坐骨神経のミエリン崩壊とマクロファージの出現（KB染色）．I：後根神経節の長期培養により樹立した不死化シュワン細胞株にみられる封入体の電顕像

J～K：Fabry病モデルマウス．J：視床にみられる血管周囲のceramide trihexoside（CTH）免疫染色像．K：後根神経節のCTH蛍光免疫染色像．L：後根神経節初代培養におけるCTH蛍光免疫染色陽性のニューロン（←），シュワン細胞（◀）

Gaucher病

Acid β-glucosidase（glucocerebrosidase）の欠乏により，glucocerebrosideが蓄積する疾患であり，肝脾腫を呈し，肝臓，脾臓，骨髄などにglucocerebrosideを貯めたPAS陽性マクロファージ（Gaucher細胞）が多数出現する．電顕的には，Gaucher細胞の細胞質にはMCBsとは異なる管状封入体を認める．Ⅰ型（成人型：慢性非神経型），Ⅱ型（乳幼児型：急性神経型），Ⅲ型（若年型：亜急性神経型）に分類され，Ⅱ型では大脳，脳幹の神経細胞の変性脱落とGaucher細胞の著明な浸潤がみられる．また，一部にパーキンソニズムを呈しα-synuclein陽性のLewy小体様封入体を海馬に認める症例が見出されている[9]．Glucocerebrosidase遺伝子ノックアウトマウスは，生後24時間以内に死亡する．

Krabbe病

Galactocerebrosidase（galactosylceremidase）の欠損により，中枢・末梢神経系のミエリン形成細胞であるオリゴデンドロサイトとシュワン細胞の変性，細胞死をひきおこす疾患であり，主として，白質の血管周囲にgalactosylceramideを蓄積したグロボイド細胞（globoid cells）をみることから，globoid cell leukodystrophy（GLD）ともよばれる．しかし脳全体としては，galactosylceramideの異常蓄積はなく，代りに中間代謝産物であるgalactosylsphingosine（psychosine）が蓄積し，これがミエリン形成細胞に毒性を示すものと理解されている．

病変は神経系に限られ，脳は萎縮しミエリンおよびオリゴデンドロサイトの変性消失と強いグリオーシス，PAS陽性のグロボイド細胞の浸潤が特徴的である．電顕的にはグロボイド細胞の胞体にgalactosylceramideからなる管状封入体を認める．末梢神経には髄鞘の消失と管状封入体を容れたマクロファージ，シュワン細胞が認められる．Krabbe病モデルマウスとしてtwitcherマウスがあり，ヒトKrabbe病とほぼ同様の表現系を示し，galactocerebrosidase遺伝子変異が同定されている（図-G～I）[10)～13)]．

Fabry病

α-galactosidase Aの欠乏によりceramide trihexoside（以下，CTHと略す）が蓄積する疾患でX染色体劣性遺伝形式をとる．心臓，肝臓，膵臓，腎泌尿器系をはじめとする全身諸臓器，血管内皮，平滑筋，また脳神経系では扁桃核，視床下部，海馬，脳幹部神経核，自律神経節，末梢神経にCTH蓄積による空胞化した細胞を認める．血管病変は脳神経系にも明らかで，脳虚血，脳梗塞や末梢神経障害をおこす．末梢神経線維は減少し，シュワン細胞にもCTH蓄積をみる．電顕的にはMCBsやzebra bodiesなどさまざまな形態を呈するものがみられる．α-galactosidase A遺伝子ノックアウトマウスでは肝臓，腎臓，脳血管，末梢神経節に同様のCTH蓄積を認める（図-J～L）[14)]．

異染性ロイコジストロフィー（metachromatic leukodystrophy）

Arylsulfatase Aの欠乏により，中枢・末梢神経系および腹部臓器にsulfatideが蓄積する疾患で，蓄積物質がトルイジン・ブルー（以下，TBと略す）染色で異染性（metachromasia）を示す．中枢神経系の広汎な脱髄を認め，TB染色で褐色に染まる細胞内顆粒を有するマクロファージと強いグリオーシスが特徴であり，同様の異染性顆粒はニューロンにもみられる．電顕的には，封入体はガングリオシドーシスに類似するMCBsからなる．末梢神経系にも脱髄がみられ，マクロファージとシュワン細胞に異染

性顆粒を認める．Arylsulfatase A遺伝子ノックアウトマウスが作られているが，予想に反して広汎な脱髄は示さない[15]．

●文　献

1) Matsuda J, Suzuki O, Oshima A et al.: Chemical chaperone therapy for brain pathology in G (M1)-gangliosidosis. Proc Natl Acad Sci USA 100: 15912-15917, 2003
2) Sango K, Yamanaka S, Hoffmann A et al.: Mouse models of Tay-Sachs and Sandhoff diseases differ in neurologic phenotype and ganglioside metabolism. Nat Genet 11: 170-176, 1995
3) Sango K, Yamanaka S, Ajiki K et al.: Lysosomal storage results in impaired survival but normal neurite outgrowth in dorsal root ganglion neurons from a mouse model of Sandhoff disease. Neuropathol Appl Neurobiol 28: 23-34, 2002
4) Murata M, Kotani M, Tajima Y et al.: Establishment of immortalized Schwann cells from a Sandhoff mouse and corrective effect of recombinant human β-hexosaminidase A on the accumulated GM2 ganglioside. J Hum Genet 50: 460-467, 2005
5) Horinouchi K, Erlich S, Perl DP et al.: Acid sphingomyelinase deficient mice: a model of types A and B Niemann-Pick disease. Nat Genet 10: 288-293, 1995
6) Saito Y, Suzuki K, Hulette CM et al.: Aberrant phosphorylation of alpha-synuclein in human Niemann-Pick type C1 disease. J Neuropathol Exp Neurol 63: 323-328, 2004
7) Watabe K, Ida H, Uehara K et al.: Establishment and characterization of immortalized Schwann cells from murine model of Niemann-Pick disease type C (spm/spm). J Peripher Nerv Syst 6: 85-94, 2001
8) Watabe K, Sakamoto T, Kawazoe Y et al.: Tissue culture methods to study neurological disorders: Establishment of immortalized Schwann cells from murine disease models. Neuropathology 23: 64-74, 2003
9) Sidransky E: Gaucher disease: complexity in a "simple" disorder. Mol Genet Metab 83: 6-15, 2004
10) Shen JS, Watabe K, Ohashi T et al.: Intraventricular administration of recombinant adenovirus to neonatal twitcher mouse leads to clinicopathological improvements. Gene Ther 8: 1081-1087, 2001
11) Shen J-S, Watabe K, Meng XL et al.: Establishment and characterization of spontaneously immortalized Schwann cells from murine model of globoid cell leukodystrophy (Twitcher). J Neurosci Res 68: 588-594, 2002
12) Meng X-L, Shen J-S, Watabe K et al.: GALC transduction leads to morphological improvement of the twitcher oligodendrocytes in vivo. Mol Genet Metab 84: 332-343, 2005
13) Shen J-S, Meng X-L, Yokoo T et al.: Widespread and highly persistent gene transfer to the CNS by retrovirus vector *in utero*: Implication for gene therapy to Krabbe disease. J Gene Med 7: 540-551, 2005
14) Sakuraba H, Chiba Y, Kotani M et al.: Corrective effect on Fabry mice of yeast recombinant human alpha-galactosidase with N-linked sugar chains suitable for lysosomal delivery. J Hum Genet 51: 341-352, 2006
15) Hess B, Saftig P, Hartmann D et al.: Phenotype of arylsulfatase A-deficient mice: relationship to human metachromatic leukodystrophy. Proc Natl Acad Sci USA 93: 14821-14826, 1996

著者連絡先

〒183-8526　東京都府中市武蔵台2-6
東京都神経科学総合研究所
渡部和彦

症例報告

両側難聴で発症した脳幹・小脳梗塞の1例
—聴性脳幹反応の経時的観察による難聴の責任病巣の考察—

角南英子* 永山寛 山崎峰雄 勝又俊弥
片山泰朗

要旨 両側性の難聴を呈し，両側小脳および脳幹に梗塞巣を認めた症例を経験した。症例は56歳男性。浮動性眩暈，歩行障害，両側難聴，耳鳴にて発症。頭部MRI上，両側中小脳脚，両側小脳半球，右大脳脚に拡散強調画像にて高信号病変を認め，頭頸部の3D–CTアンギオでは，両側椎骨動脈に高度の狭窄を認めた。第14病日の聴性脳幹反応(ABR)では，両側ともII波からV波まで消失していたが，第61病日にはI波からV波まで全波が認められた。ABRの結果から，難聴の責任病巣として，橋下部聴神経線維のほか，蝸牛神経の障害が推定された。既報告例と同様に，本症例の難聴の予後は比較的良好であったが，その原因として，本症例が高度の両側椎骨動脈狭窄を基盤とした血行力学的機序によって起きた脳梗塞であり，梗塞部位への側副血行路からの血流が，可逆的な聴力変化をもたらした可能性が考えられた。

Key words：bilateral hearing loss, brainstem infarction, anterior inferior cerebellar artery, auditory brain stem responses

はじめに

難聴を呈する脳梗塞としては，聴神経を支配する前下小脳動脈や上小脳動脈領域の梗塞や側頭葉皮質聴覚野の梗塞が知られている。しかし，両側難聴をきたした脳梗塞は稀であり，詳細な報告例は少ない[1–5]。今回われわれは，両側難聴を呈し，小脳および脳幹に梗塞巣を認め，難聴改善の経過をABRで経時的にフォローアップしえた症例を報告する。

症　例

症　例　56歳，男性

主　訴　両側難聴，浮動性眩暈，歩行障害，耳鳴

家族歴　母，高血圧症，脳出血のため35歳で死亡。妹，脳出血のため50歳で死亡。

既往歴　20歳台より高血圧指摘されるも無治療，47歳でくも膜下出血。

嗜　好　タバコ20本／日，飲酒せず

現病歴　2004年2月某日(第1病日)15時頃，浮動性眩暈，歩行障害が出現。同日19時に嘔吐あり，20時テレビを見ているときに両側難聴と耳鳴りが出現し，音がまったく聞こえなくなった。第5病日朝，歩行障害の増悪を認めたため，当院耳鼻科を受診するが，脳梗塞の疑いで当科に紹介となり，入院となった。

入院時一般身体所見　血圧152/84 mmHg，脈拍74/分整，体温36.7℃。胸部聴診上心雑音および肺雑音なし。

入院時神経学的所見　意識は清明。脳神経系は，視力視野障害はなく，瞳孔左右差を認めず，対光反射正常であった。眼球運動障害なく，左右の注視方向性水平性眼振を認めた。顔面に左右差なく，感覚障害と運動障害を認めなかった。両側に高度の感音性難聴と耳鳴，浮動性眩暈を認めた。失調性構音障害を認めたが，嚥下障害や舌偏位は認めなかった。深部反射は異常なく，病的反射を認めなかった。運動系では左上肢Barré徴候陽性で，左上肢MMTは4/5程度であった。下肢には運動麻痺を認めなかった。感覚系では表在覚，深部覚共に異常を認めなかった。協調運動は指鼻試験および膝踵試験が両側拙劣であり，両側測定障害を認めた。歩行は開脚失調性歩行であった。

検査所見　血液生化学検査では軽度の高脂血症以外，血算，生化学，凝固・血小板系マーカーにおいては明

* 日本医科大学付属病院第2内科(2005年11月22日受稿)
〔連絡先〕角南英子：日本医科大学付属病院第2内科(〒113–8603 東京都文京区千駄木1–1–5)

0006–8969/06/¥500/論文/JCLS

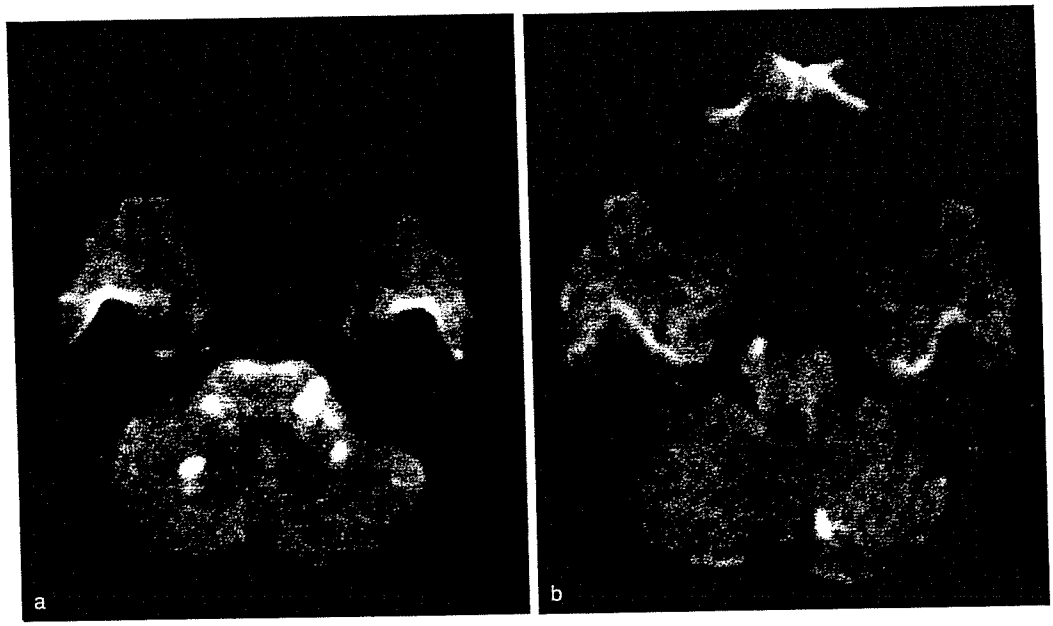

Fig. 1 Diffusion weighted image (DWI) on day 6
a : DWI showed high signals in the dorsolateral pons, bilateral middle cerebellar peduncles and bilateral cerebellar hemispheres at mid-pontine level. **b** : DWI showed high signals in the right cerebral peduncle and the cerebellar hemisphere at midbrain level.

らかな異常を認めなかった。心電図では洞調律であり，経食道心エコーでは右左シャントを伴う卵円孔の開存を認めるものの，明らかな心内血栓を認めなかった。また，下肢RIベノグラフィーおよび肺血流シンチにて，深部静脈血栓や肺塞栓を疑う所見を認めなかった。

画像所見 第6病日の頭部MRIにて，右大脳脚，両側橋背外側部，両側中小脳脚，両側小脳半球に拡散強調画像(DWI)，T2強調像にて高信号を示す梗塞巣を認めた(Fig. 1-a, b)。また，左中脳にT2高信号域を認め，陳旧性虚血巣と考えられた。テント上には虚血巣を示唆するT2延長域は目立たなかった。また，MRAでは椎骨動脈，脳底動脈および両側後大脳動脈の描出なく(Fig. 2)，第17病日の頭頸部3D-CTAでは椎骨脳底動脈系は描出されたが，両側の椎骨動脈に高度の狭窄を認め(Fig. 3)，両側椎骨動脈は，大後頭孔レベルより中枢側で，描出不良であった。頸動脈エコーでは，椎骨動脈径は両側とも細く，特に左側は血流評価困難であった。SPECTでは，左側頭皮質から一部前頭皮質に至る部位と小脳で血流低下を認めた。

神経耳科検査 入院時(第5病日)のオージオメーターでは，4分法で右90 dB，左80 dBの感音性難聴を認めた。第15病日には右69 dB，左56 dBに改善したが，第42病日，第64病日とほぼ横ばいであった。また，第14病日のABRでは，両側ともI波のみを認め，I波潜時は左側では正常，右側では延長していた(Fig. 4-a)。第42病日には，左側で，II波，右側でI，II，V波を認めた。両側のI，II波潜時は正常であったが，右V波の潜時は延長していた(Fig.4-b)。第61病日にはすべての波を認めたが，右側では，III波以降の潜時と，I-III波頂点間潜時の延長を認めた(Fig. 4-c)。

経 過 第5病日に入院し，オザグレル 160 mg/日，グリセロール 400 ml/日にて治療を開始した。第6病日に新たに右顔面のしびれ感が出現し，症状が進行性であったため，オザグレルからアルガトロバンに変更投与し，エダラボン 60 mg/日を併用とした。第12病日にシロスタゾール200 mg/日を内服開始した。聴力は早期より改善傾向を示し，日常会話可能となった。難聴以外の神経症状も軽快し，第57病日に杖歩行で退院した。

考 察

本症例は浮動性眩暈と歩行障害にて発症，その後両側性の難聴，耳鳴りを認め，症状が階段状に増悪した。当初耳鼻科を受診したが，小脳失調を伴うため脳梗塞が疑われ，神経内科に入院した。MRIにて両側の中小脳脚，両側小脳半球，右大脳脚に梗塞巣を認めた。

中小脳脚は，解剖学的に前下小脳動脈(AICA)だけ

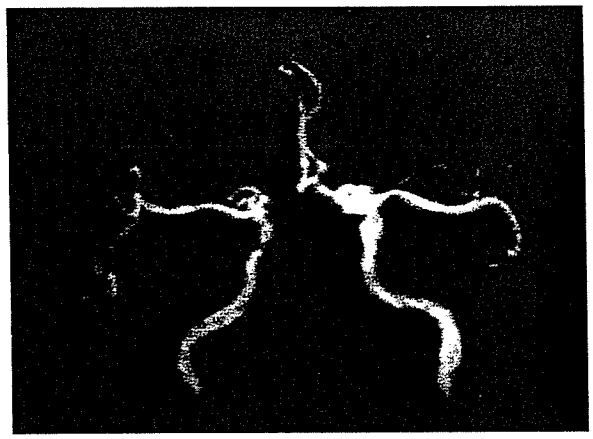

Fig. 2 Magnetic resonance angiography (MRA) on day 6
MRA showed disappearance of bilateral vertebral arteries, basilar artery, and bilateral posterior cerebral arteries.

Fig. 3 3D-CT angiography (3D-CTA) on day 17
3D-CTA showed severe stenosis of bilateral vertebral arteries.

でなく，上小脳動脈(SCA)からも灌流をうけており[6]，分水嶺領域と理解されている。また，本症例における両側小脳半球の梗塞部位は，小脳髄体にあり，AICAおよびSCAの分水嶺に相当する。本症例の梗塞部位はほぼ左右対称性であり，両側椎骨動脈の高度の狭窄を基盤とした，血行力学性機序によるAICAとSCAの分水嶺梗塞の可能性が考えられた。なお，検査結果から心原性脳塞栓症，動脈解離は否定的であった。また，奇異性脳塞栓症については，卵円孔開存を認めたものの，下肢RIベノグラフィーおよび肺血流シンチにて，深部静脈血栓や肺塞栓を疑う所見を認めず，積極的には疑れなかった。

両側難聴を呈した脳幹部梗塞の既報告全例で本症例と同様に，両側もしくは一側の橋，中小脳脚に梗塞巣を認め[1-5]，ほとんどの症例で椎骨脳底動脈に動脈硬化による高度な狭窄または閉塞があり，椎骨脳底動脈の循環不全が発症に関与していると考えられた。

本症例における難聴の成立機序については，中小脳脚，橋下部背外側の梗塞により，脳幹部聴神経線維(台形体，外側毛体)が障害され，中枢性の難聴をきたした可能性が考えられるほか，AICA灌流域である蝸牛神経核，蝸牛神経線維の障害による末梢性難聴の可能性も考えられる。本症例では，ABRを経時的に3回施行し，聴力の改善と共にABRの回復過程を追跡し，その結果から難聴の責任病巣を推測した。

第14病日のABRでは，両側ともI波のみが認められた。左側ではII波以降が消失していることから，蝸牛神経近位部や蝸牛神経核より中枢側の障害が示唆された。一方右側では，I波潜時は延長しており，より末梢側での障害が考えられた。第42病日では，両側ともI波，II波を認め，潜時も正常であり，蝸牛神経から蝸牛神経核領域の回復が示唆された。第61病日には，両側にて全波が認められたが，右側でIII波以降の潜時が延長しており，橋下部聴覚神経線維の障害が残存すると考えた。

両側難聴を呈した脳幹部梗塞の従来の報告で，ABRにて末梢性難聴を示す例と中枢性難聴を示す例があり[1,2,7]，本症例も両方の機序が混在する可能性が示された。

本症例では，ABRの改善に先行して，第15病日には聴力の著明な改善を認めている。両側難聴を呈する脳幹部梗塞では，本症例と同様，聴力は比較的早期に改善し予後良好であることが特徴と考えられる[1-3]。しかし，その原因は明らかではない。本症例は，血行力学性機序によって起きたために，虚血が不完全で，さらに，AICAは同側の後下小脳動脈(PICA)やSCAを介した側副血行の発達が良好なため[8]，梗塞部位への側副血行路からの血流が，可逆的な聴力変化を持たらせたと推測される。

ところで，本症例は，浮動性眩暈および歩行障害にて発症しているが，初期症状が難聴のみの症例もあり[1]，その場合，突発性難聴などの内耳疾患との鑑別が困難である。Leeらは，突発する難聴は，AICA領域梗塞の前駆症状として重要であることを指摘し，前

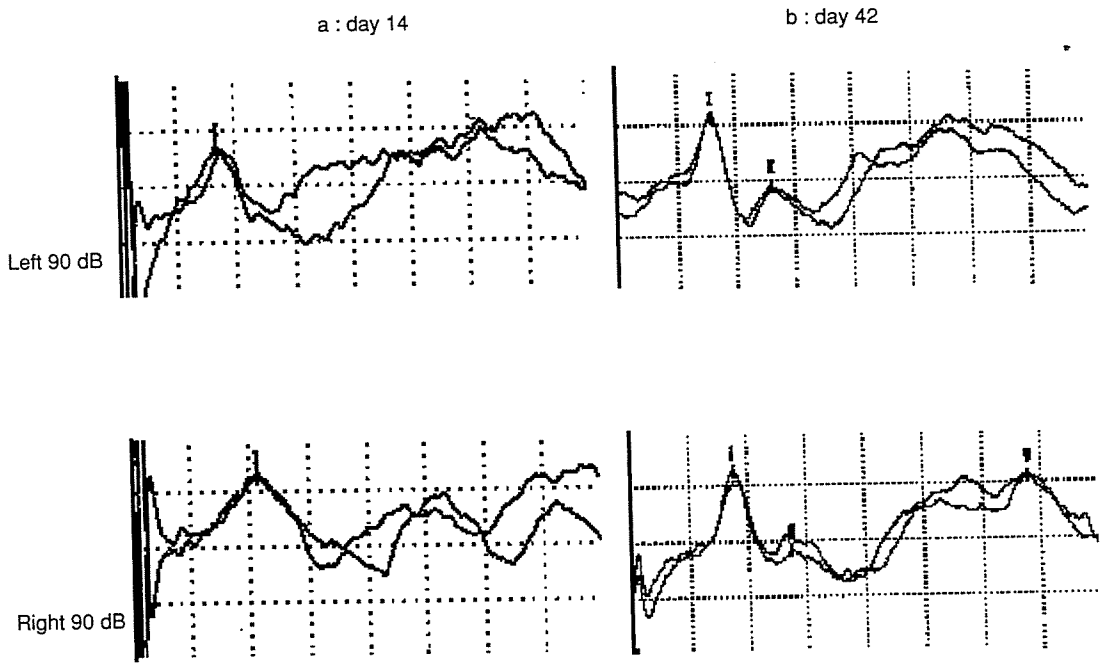

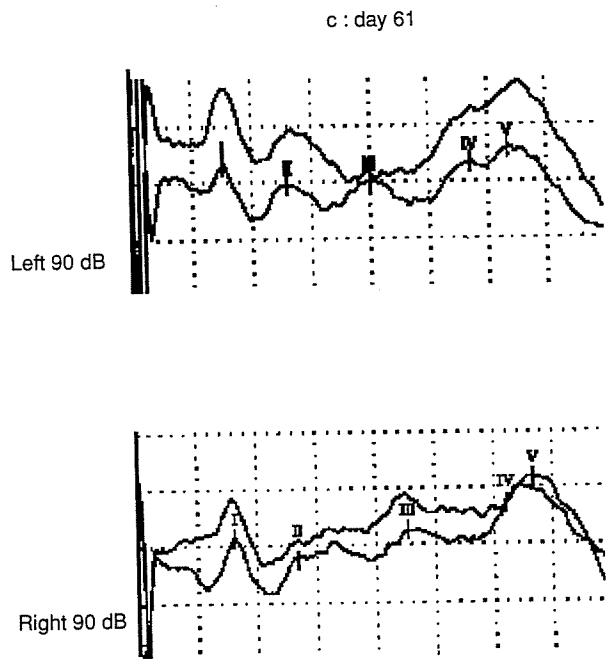

Fig. 4 Auditory brain stem response (ABR)
a : ABR on day 14 showed normal wave I and absence of waves II–V on the left ; prolonged wave I peak latency and absence of waves II–V on the right. **b** : ABR on day 42 showed normal waves I and II on both sides, and prolonged wave V peak latency on the right. **c** : ABR on day 61 showed all waves on the both sides, but waves III, IV and V peak latencies and I–III interpeak interval on the right were prolonged.

駆症状として出現する難聴は，AICAの終末動脈である内耳動脈の虚血によるものであることを指摘している[9,10]。

突発する両側難聴をきたす脳梗塞では，背景に椎骨脳底動脈の高度の血管病変が存在し，階段状に症状が増悪するが，難聴の予後は比較的良好であることが特徴であると考えられた。

文　献

1) 市川博雄, 福井俊哉, 根岸晶子, 杉田幸二郎, 神田実喜男：両側性突発性難聴で発症した両側小脳脚部梗塞の1例. 臨床神経 34：569–575, 1994
2) 崎川康彦, 工藤葉子, 渡辺尚彦, 野村恭也：両側難聴で発症した小脳梗塞症例. Otol Jpn 4：67–73, 1994
3) 小林久滋, 杉原　浩, 米山公啓, 清水　亨, 加藤　功：両側難聴で初発した脳幹梗塞. 神経内科 40：188–190, 1994
4) Lee H, Whitman GT, Lim JG, Park YC：Bilateral sudden deafness as a prodrome of anterior inferior cerebellar artery infarction. Arch Neurol 58：1287–1289, 2001
5) Toyoda K, Hirano T, Kumai Y, Fujii K, Kiritoshi S, Ibayashi S：Bilateral deafness as a prodromal symptom of basilar artery occlusion. J Neurol Sci 193：147–150, 2002
6) Carpenter MB：Human Neuroanatomy. 7 th ed, Williams & Wilkins Company, Baltimore, p621, 1976
7) Huang MH, Huang CC, Ryu SJ, Chu NS：Sudden bilateral hearing impairment in vertebrobasilar occlusive disease. Stroke 24：132–137, 1993
8) 高松和弘, 大田泰正：前下小脳動脈(AICA)症候群. 神経内科 46：350–358, 1997
9) Lee H, Sohn SI, Jung DK, Cho YW, Lim JG, Yi SD, Lee SR, Sohn CH, Baloh RW：Sudden deafness and anterior inferior cerebellar artery infarction. Stroke 33：2807–2812, 2002
10) Lee H, Cho YW：Auditory disturbance as a prodrome of anterior inferior cerebellar artery infarction. J Neurol Neurosurg Psychiatry 74：1644–1648, 2003

Abstract

A Case of Infarction in Brainstem and Cerebellum as a Initial Symptom with Bilateral Hearing Loss

by

Eiko Sunami*, Hiroshi Nagayama, Mineo Yamazaki, Toshiya Katsumata, Yasuo Katayama

from

* The Second Department of Internal Medicine, Nippon Medical School, 1-1-5 Sendagi, Bunkyo-ku, Tokyo 113-8603, Japan

A 56-year old male presented with a sudden onset of bilateral hearing difficulty. He complained of dizziness and gait disturbance at the onset and subsequently developed bilateral hearing loss and tinnitus. Brain MRI revealed multiple infarcts in bilateral middle cerebellar peduncles, bilateral cerebellar hemispheres and the right cerebral peduncle. Three dimentional computed tomography angiography (3D-CTA) showed severe stenosis of bilateral vertebral arteries. Infarcts were located in the border zone between anterior inferior cerebellar artery (AICA) and superior cerebellar artery (SCA), suggesting hemodynamic infarctions. Auditory brain stem responses (ABR) were recorded three times. The initial ABR demonstrated all waves except for wave I on day 14. Wave I on the left was normal, while wave I peak latency on the right was prolonged. On day 61, all waves were recorded, although peak latencies of waves III to V and interpeak intervals of the wave I to III on the right side were prolonged. Involvements of the cochlear nerve and pontine auditory pathway were suggested from the ABR abnormalities in this case.

(Received : November 22, 2005)

Journal of Neurochemistry, 2006, **99**, 70–83 doi:10.1111/j.1471-4159.2006.04021.x

Hepatoma-derived growth factor, a new trophic factor for motor neurons, is up-regulated in the spinal cord of PQBP-1 transgenic mice before onset of degeneration

Shigeki Marubuchi,*,† Tomohiro Okuda,† Kazuhiko Tagawa,* Yasushi Enokido,* Daisuke Horiuchi,* Reiko Shimokawa,* Takuya Tamura,* Mei-Ling Qi,* Yoshinobu Eishi,# Kazuhiko Watabe,‡ Masao Shibata,§ Masaya Nakagawa† and Hitoshi Okazawa*,¶

**Department of Neuropathology, Medical Research Institute and 21st Century Center of Excellence Program for Brain Integration and Its Disorders, Tokyo Medical and Dental University, Tokyo, Japan*

†Toyama Chemical Co., Ltd, Toyama, Japan

#Department of Pathology, Tokyo Medical and Dental University, Tokyo, Japan

‡Tokyo Metropolitan Institute for Neuroscience, Tokyo, Japan

§MBL Co. Ltd, Nagano, Japan

¶PRESTO, Japan Science and Technology Agency, Saitama, Japan

Abstract

Hepatoma-derived growth factor (HDGF) is a nuclear protein homologous to the high-mobility group B1 family of proteins. It is known to be released from cells and to act as a trophic factor for dividing cells. In this study HDGF was increased in spinal motor neurons of a mouse model of motor neuron degeneration, polyglutamine-tract-binding protein-1 (PQBP-1) transgenic mice, before onset of degeneration. HDGF promoted neurite extension and survival of spinal motor neurons in primary culture. HDGF repressed cell death of motor neurons after facial nerve section in newborn rats *in vivo*. We also found a significant increase in p53 in spinal motor neurons of the transgenic mice. p53 bound to a sequence in the upstream of the *HDGF* gene in a gel mobility shift assay, and promoted gene expression through the *cis*-element in chloramphenicol acetyl transfer (CAT) assay. Finally, we found that HDGF was increased in CSF of PQBP-1 transgenic mice. Collectively, our results show that HDGF is a novel trophic factor for motor neurons and suggest that it might play a protective role against motor neuron degeneration in PQBP-1 transgenic mice.

Keywords: degeneration, motor neuron, polyglutamine, polyglutamine-tract-binding protein-1, trophic factor.
J. Neurochem. (2006) **99**, 70–83.

Hepatoma-derived growth factor (HDGF) was originally purified from the conditioned medium of the human hepatoma-derived cell line, HuH7, by monitoring the growth-stimulating activity on Swiss 3T3 cells (Nakamura *et al.* 1994). Molecular cloning of the cDNA revealed that HDGF is homologous (32% in amino acid sequences) to high mobility group protein-B1 (HMGB1) (Nakamura *et al.*

Received March 9, 2006; revised manuscript received May 11, 2006; accepted May 22, 2006.

Address correspondence and reprint requests to Hitoshi Okazawa, Department of Neuropathology, Tokyo Medical and Dental University, 1-5-45, Yushima, Bunkyo-ku, Tokyo 113-8510, Japan.
E-mail: okazawa-tky@umin.ac.jp

Abbreviations used: ALS, amylotrophic lateral sclerosis; BDNF, brain-derived neurotrophic factor; bFGF, basic fibroblast growth factor; CAT, chloramphenicol acetyl transfer; ChAT, choline acetyltransferase; CNTF, ciliary neurotrophic factor; Cont, control; DMEM, Dulbecco's modified Eagle's medium; E*n*, embryonic day *n*; GAPDH, glyceraldehyde-3-phosphate-dehydrogenase; GFAP, glial fibrillary acidic protein; GST, glutathione transferase; HDGF, hepatoma-derived growth factor; HEK, human embryonic kidney; HMG, high-mobility group; IFN, interferon; IL, interleukin; JNK, c-Jun N-terminal kinase; MMLV, Moloney murine leukemia virus; PBS, phosphate-buffered saline; PC, phase contrast; PQBP, polyglutamine tract-binding protein-1; RAGE, receptor for advanced glycation end-products; SDS, sodium dodecyl sulfate; SSC, saline sodium citrate buffer; SOD, superoxide dismutase; Tg, transgenic.

1994), although HDGF lacks the HMG box, a DNA-binding domain shared by HMG proteins. HDGF contains a nuclear localization signal sequence, and it is actually located in the nucleus (Kishima *et al.* 2002). On the other hand, HDGF is released from cells in a similar manner to the way in which HMGB proteins are released in necrosis (Scaffidi *et al.* 2002). The released HDGF promotes proliferation of fibroblasts, HuH7 cells (Nakamura *et al.* 1989), endothelial cells (Oliver and Al-Awqati 1998) and smooth muscle cells (Everett *et al.* 2000). These findings collectively suggest that HDGF is a growth factor involved in the tissue damage response.

We have investigated molecular mechanisms underlying neurodegeneration of polyglutamine diseases and have found a candidate mediator molecule of the pathology, polyglutamine-tract-binding protein-1 (PQBP-1) (Waragai *et al.* 1999; Okazawa *et al.* 2002). Interestingly, transgenic (Tg) mice overexpressing PQBP-1 show a late-onset motor neuron disease phenotype (Okuda *et al.* 2003). We performed microarray analysis of gene expression profiles in PQBP-1 Tg mice and reported that a major group of changed genes are those transcribed from the mitochondrial genome (Marubuchi *et al.* 2005). Simultaneously, we found up-regulation of HDGF in the spinal cord of PQBP-1 Tg mice, and analyzed the pathophysiological significance in this study.

Western blot and immunohistochemistry showed that HDGF is increased in the nuclei of motor neurons of presymptomatic PQBP-1 Tg mice. HDGF had trophic effects on motor neurons in our analyses with primary motor neurons and facial motor neurons after nerve section. In addition, p53, which was increased in spinal motor neurons of PQBP-1 Tg mice, activated transcription from the *HDGF* gene through binding sites in the upstream region. Furthermore, HDGF was increased in the CSF of these Tg mice. Collectively, these results suggest that HDGF might be a new motor neuron trophic factor that plays a protective role against motor neuron degeneration in PQBP-1 Tg mice.

Materials and methods

Total RNA preparation

For each microarray analysis, spinal cords at the level from L1 to L2 were removed from three PQBP-1 Tg mice or from three age-matched littermates at 2 and 12 months. The anterior halves of the spinal cords were dissected using razor blades under microscopy. Dissected tissues from each group were transferred into a glass homogenizer and homogenized with Trizol reagent (Invitrogen, Carlsbad, CA, USA). Total RNA was prepared according to the manufacturer's protocol.

Cy3- or Cy5- labeled amplified RNA preparation for microarray analyses

Labeling and amplification of RNA was performed using the Agilent Fluorescent Linear Amplification kit (Agilent Technologies, Palo Alto, CA, USA) according to the manufacturer's protocol. First, double-stranded cDNAs with T7 promoter were synthesized from 2 μg total RNA by Moloney murine leukemia virus (MMLV) reverse transcriptase using oligo dT primer, which contains the T7 promoter sequence, and random hexamers (40°C, 4 h). Then, using these double-stranded cDNAs as templates, cRNA was synthesized by T7 RNA polymerase using Cy3- or Cy5- labeled CTP (40°C, 1 h). cRNAs from PQBP-1 Tg mouse and age-matched littermates were labeled with Cy3 and Cy5 respectively. Synthesized cRNA was precipitated with lithium chloride, rinsed with ethanol and dissolved in nuclease-free water. To check the quality of cRNA, OD_{260}, OD_{280}, A_{552} (for Cy3) and A_{650} (for Cy5) were measured. Then, OD_{260}/OD_{280}, amplification rate and dye incorporation rate (pmol/μg RNA) of the cRNA were calculated. Our samples were of high quality based on these criteria (OD_{260}/OD_{280} 2.0 >, amplification rate 400 >, Cy3 incorporation > 15 pmol/μg RNA and Cy5 incorporation > 12 < pmol/μg RNA). Microarray analysis with the mixture of total RNA from three mice was repeated twice.

Hybridization of microarrays

Hybridization procedures were performed using *In Situ* Hybridization Plus kit (Agilent Technologies) according to the manufacturer's manual. First, Cy3- and Cy5- labeled cRNAs (1 μg each) were mixed and incubated with fragmentation buffer (Agilent Technologies) at 60°C for 30 min. Then, Mouse Development Oligo Microarray (Agilent technologies), which contains 20 371 60mer oligonucleotides from mouse cDNA, was hybridized with fragmented cRNA target at 60°C for 17 h. Hybridized microarrays were rinsed twice and dried by spraying N_2 gas (99.999%) using a filter-equipped air-gun (Nihon mycrolis KK, Tokyo, Japan).

Signal detection and data analysis of microarrays

The fluorescence signal was read using a microarray scanner, CRBIO® IIe (Hitachi Software Engineering Co., Ltd, Tokyo, Japan). Data were analyzed using the software DNASIS® array (Hitachi Software Engineering Co., Ltd). Briefly, data either from control spots or from spots containing high intensities of artificial signals were removed. Then, the signal intensity of each spot was normalized to equalize total signal intensity. The normalized signal intensity of each spot was plotted on a scatter plot with Cy3 fluorescence on the *y*-axis, and Cy5 fluorescence on the *x*-axis. The ratio of Cy3 fluorescence (gene expression in PQBP-1 Tg mice) to Cy5 fluorescence (gene expression in age-matched littermates) were calculated, and genes with a Cy3/Cy5 ratio of more than 1.5 or less than 0.67 were listed (Marubuchi *et al.* 2005). To identify genes of interest, the sequences of 60mer oligonucleotides on the spots of interest were retrieved from Agilent Technology and the sequences were searched for in a mouse cDNA database using National Center for Biotechnology Information at NIH (NCBI) BLAST. Most of the selected spots of interest were identified with aid of the manufacturer's annotation information, although there were several unidentified genes.

Northern blot analysis

Northern blot analysis was performed basically as described previously (Okamoto *et al.* 1990; Okazawa *et al.* 1991). Some 15 μg total RNA was separated on a 1% agarose gel and blotted to Hybond-N (Amersham Biosciences, GE Health Care BioSciences,

Kwai Chung, Hong Kong). Hybridization was performed in 5 × saline sodium citrate buffer (SSC) containing 0.5% sodium dodecyl sulfate (SDS), 5 × Denhardt's solution and 20 μg/mL salmon sperm DNA at 60°C for 24 h. The membrane was washed twice in 2 × SSC–0.1% SDS at 50°C for 20 min and twice in 0.1 × SSC–0.1% SDS at 55°C for 20 min. The membrane was exposed to Hyperfilm ECL (Kodak, New York, USA) for 72 h.

Generation of antibody against HDGF

An antiserum against HDGF was raised by immunizing rabbits with the peptide KEEAEAPGVRDHESL (C-terminal 15 amino acids of mouse HDGF) or with the peptide KEDAEAPGIRDHESL (C-terminal 15 amino acids of human HDGF) conjugated to the carrier protein by cysteine. The specificity of these antibodies in western blot and immunohistochemistry was reconfirmed by preabsorption with glutathione transferase (glutathione S-transferase [GST])-HDGF (data not shown).

Immunohistochemistry

PQBP1 Tg and control mice at 7, 16 and 20 months were transcardinally perfused with cold 4% paraformaldehyde. The brains and the spinal cords were post-fixed in 4% parafolmaldehyde for 24 h. Paraffin sections (5–10 μm) were de-paraffinized in xylene and rehydrated through an ethanol dilution series. Endogenous peroxidase was inactivated with 0.3% hydrogen peroxide in phosphate-buffered saline (PBS) for 30 min. Paraffin sections were treated with 3% goat serum for 30 min. For HDGF staining, anti-HDGF C-terminal polyclonal rabbit serum (1 : 1000 dilution) with or without anti-glial fibrillary acidic protein (GFAP) rabbit polyclonal antibody (1 : 500; Chemicon, Temecula, CA, USA) was used as primary antibody. For p53 staining, p53 rabbit polyclonal antibody (Santa Cruz Biotechnology Inc., Santa Cruz, CA, USA) was used at 1 : 100 dilution and another rabbit polyclonal anti-p53 antibody (CM5; Novocastra) was used at 1 : 200 dilution. Horseradish peroxidase-conjugated anti-rabbit antibody (Envision; DAKO, Glostrup, Denmark) was used as a secondary antibody according to the protocol and visualized with diaminobenzidine (Sigma, St Louis, MO, USA). Antibodies against phospho-p53 at Ser15, Ser20 or Ser389 (Cell Signaling, Beverly, MA, USA) were diluted at 1 : 200 and used for immunohistochemistry. The first two antibodies did not show any signal in the spinal cord of control and Tg mice.

Generation and purification of recombinant HDGF

To express GST-HDGF fusion protein, full-length mouse HDGF cDNA amplified by PCR with the primers HDGF-F (AAAGGGATCCGATCCAACCGGCAGAAAGAG) and HDGF-R (AAAGAATTCTACAGGCTCTCATGATCTCT) was subcloned between *Bam*HI and *Eco*RI restriction sites of pGEX-3X (Amersham Biosciences). As a result of this subcloning the first two N-terminal amino acids of HDGF were changed from M-S to G-I. After 5 h of induction with Isopropyl-beta-D-thiogalactoside (IPTG) at 0.1 mM, *Escherichia coli* cells were collected by centrifugation and sonicated. GST-HDGF was recovered from the lysate using a glutathione sepharose 4B column (Amersham Biosciences). HDGF was cleaved from the fusion protein by Factor Xa, and purified with a heparin-sepharose column (HiTrap Heparin HP; Amersham Biosciences).

Spinal cord tissue culture and analyses of neurite outgrowth

Spinal cords of embryonic day 14 (E14) Sprague–Dawley rat embryos were dissected and dorsal root ganglia and meninges were stripped away. The ventral half of the spinal cord was separated under the microscope and cut into a 1-mm cube of tissue, whereas the dorsal half of the spinal cord was discarded. The ventral tissue was plated on to a poly-L-lysine-coated 35-mm dish (Falcon, BD Biosciences, San Jose, CA, USA) which had been incubated overnight with Dulbecco's modified Eagle's medium (DMEM), and cultured in 5% CO_2 at 37°C. Three HDGF concentrations, 3, 10 and 30 ng/mL, were examined for neurite-promoting activity, and 6–10 explants were used at each concentration. The culture medium was exchanged every other day. Neurite outgrowth of explants was evaluated after 7 days by using WinROOF software (Mitani Corporation, Tokyo, Japan). For anti-choline acetyl transferase (ChAT) antibody staining, the tissues were fixed with 0.1% paraformaldehyde and incubated with goat anti-ChAT polyclonal antibody (Chemicon) at a dilution of 1 : 500 for 12–24 h at 4°C. The stain was visualized with donkey anti-goat IgG labeled with Alexa Fluor 488 (Molecular Probes, Eugene, OR, USA) and observed by fluorescence microscopy (IX-71; Olympus, Tokyo, Japan) and Aquacosmos software (Hamamatsu Photonics, Hamamatsu, Japan).

Primary culture of spinal motor neurons and analysis of survival effects

Rat embryo (E14) spinal cords were dissected, and the dorsal half of the spinal cord was removed under the microscopy. The ventral half was chopped into small pieces using razor blades, incubated in PBS containing 0.05% trypsin for 15 min at 37°C, and dissociated mechanically. After filtration, the cells were plated in 24-well plates (Greiner, Kremsmünster, Austria) that had been coated with polyornithine (Sigma) and laminin (Invitrogen) at a density of 6×10^4 cells/well. The cells were cultured in neurobasal medium (Gibco, Rockville, MD, USA) supplemented with B27 (Gibco), glutamate (Wako, Tokyo, Japan), glutamine (Wako), 3-mercapto-ethanol (Nakarai, Tokyo, Japan) and Gentamicin (Gibco). Recombinant mouse HDGF (3 or 30 ng/mL) or recombinant human BDNF (30 ng/mL; Pepro Tech, London, UK) were added to the culture medium simultaneously. Twelve hours after plating, cytosine arabinoside (Sigma) was added to the medium at 4 M final concentration. The cells were cultured at 37°C in 5% CO_2 for 7 days, fixed with 2% paraformaldehyde in 0.1 M phosphate buffer, and stained with anti-ChAT antibody (Chemicon). ChAT-positive cells were counted as motor neurons.

Facial nerve section of newborn rats and survival of facial motor neurons

The main trunk of the facial nerve was sectioned unilaterally in newborn pups (P1). The proximal nerve stump was treated with a piece of Spongel (Yamanouchi, Astellas, Tokyo, Japan) containing 5 μg HDGF in 4 μL PBS with 1% bovine serum albumin (Sigma). Human BDNF was applied in a similar manner as positive control and a piece of Spongel soaked in 4 μL PBS with 1% bovine serum albumin was implanted as a negative control. After 7 days, the animals were transcardially perfused with ice-cold 20 mL 4% paraformaldehyde in 0.1 M phosphate buffer. The brains were dissected and soaked in the similar solution for 12 h. The brainstem

was embedded in paraffin, and 6 μm-thick serial coronal plane sections were prepared using a microtome. The serial sections were stained with cresyl violet and the neurons in the facial nucleus were counted on injured and uninjured sides. The percentage of motor neurons on the injured side compared with the uninjured side was calculated in each mouse.

Primary culture of cortical neurons

Cerebral cortical tissues were isolated from E17 Wistar rat embryos, minced using razor blades, and treated with 0.25% trypsin (Gibco) in PBS (pH 7.5) at 37°C for 20 min, with gentle shaking every 5 min. After stopping the reaction with DMEM containing 50% fetal bovine serum, Dnase I (Boehringer Mannheim, Indianapolis, IN, USA) was added to the solution at a final concentration of 100 μg/mL, and tissues were dissociated gently by pipetting with blue tips. Cells filtered through nylon mesh (pore size 70 mm; Falcon) were collected by centrifugation, resuspended in DMEM supplemented with 20 mM glucose, 16 mM sodium bicarbonate, 4 mM glutamine, 25 μg/mL gentamicin and 10% fetal bovine serum, and then plated on 24-well dishes (Corning, Corning, NY, USA) coated with polylysine (Sigma) at 3×10^5 cells/well. Twelve hours after plating, cytosine arabinoside was added to the culture medium at 4 M final concentration to prevent growth of glial cells.

Construction of adenovirus vector

Adenovirus vectors for expression of PQBP-1 proteins were constructed by subcloning full-length PQBP-1 cDNA (Waragai *et al.* 1999) into the *SwaI* site of a cosmid vector, pAxCAwt (Takara, Tokyo, Japan). These cosmids were transfected into HEK 293 cells with the fragmented adenovirus DNA (DNA-TPC) by the calcium phosphate method, so that adenovirus containing the insert was generated by recombination. The transfected cells were harvested after 12 h, dissociated and cultured in 96-well collagen-coated dishes for 3 weeks. From wells in which cells showed lysis between 7 and 15 days after transfection, the medium was recovered as the primary virus solution. The solution (Ax-PQBP1) was amplified two or three times in 293 cells, and the working virus solution was prepared by sonicating the final 293 cells 3 days after transfection. We confirmed the insert in adenovirus vector by PCR before use. These steps were performed according to the protocol of Adenovirus Expression Vector kit (Takara).

Gel mobility shift assay

Gel mobility shift assay was performed as described previously (Okamoto *et al.* 1990; Okazawa *et al.* 1991). To make the probes, sense and antisense oligonucleotides of the sequences shown in Supplementary figure 2 and possessing additional 5′-GGG were synthesized, annealed and radiolabeled with [α-^{32}P]dCTP and Klenow enzyme (Takara). Some 10 000 cpm of probes were incubated with 5 ng human recombinant p53 protein that was purified by affinity chromatography and gel filtration (Active Motif, Carlsbad, CA, USA).

Chloramphenicol acetyl transfer (CAT) assay

CAT assay was performed according to the method described previously (Okamoto *et al.* 1990; Okazawa *et al.* 1991). In brief, 1×10^7 HEK293 or P19 cells were cultured in 10-cm dishes and after 12 h they were transfected with plasmids using Superfect (Qiagen, Valencia, CA, USA). Transfection efficiency was verified by pCH110 (Promega, Madison. WI, USA), a eukaryotic expression vector containing the simian virus early promoter and the *E. coli* β-galactosidase (LacZ) structural gene. After further 24 h, cells were harvested and used for CAT assay. pHDGFe2-IFN-CAT, containing the e1/2 sequence upstream of the interferon (IFN) promoter and *CAT* gene, was constructed by subcloning the region around the e2 sequence amplified by PCR between *NotI* and *XbaI* sites of pIFN-CAT (Okazawa *et al.* 1991). The PCR reaction was performed with mouse genomic DNA using the primers SF1 (CAGCGGC-CGCCTTTAAGTCAGGATCTT) and SF2 (GTTCTAGAAGGA-GCAGAAGTTCCAGGCCAT). p53 expression vector, pCI-p53, was constructed by subcloning full-length rat p53 cDNA between *EcoRI* and *SalI* sites of pCIneo (Promega).

CSF collection

CSF was collected from three Tg and three littermate mice under deep anesthesia by tapping cisterna magna with a 23-G needle.

Mutant SOD1

A human SOD1 transgenic strain, B6SJL-TgN (SOD1-G934) 1 Gu (The Jackson Laboratories) was used for morphological analyses.

Results

HDGF expression is up-regulated in the spinal cord of motor neuron degeneration model mice

PQBP-1 Tg mice show progressive weakness of hind limbs when they become more than 18 months old. Pathological analyses have revealed that motor neurons in the lumbar spinal cord are degenerated (Okuda *et al.* 2003). To understand the molecular mechanisms underlying the pathology, we analyzed gene expression in the lumbar spinal cord of presymptomatic PQBP-1 Tg mice (2 and 12 months old) using Mouse Development Oligo Microarray (Agilent Technologies). We did not perform microarray analysis with older Tg mice after the onset of symptoms because dysfunction and loss of motor neurons prevented us from getting primary changes in gene expression profiles. The probes were synthesized from RNA samples of three Tg or age-matched littermate mice, and the microarray experiments were repeated twice. We compared the expression profiles, and selected 14 genes whose expression was constantly changed more than 1.5-fold in Tg mice (Marubuchi *et al.* 2005). Thirteen genes were up-regulated whereas one gene was down-regulated. The up-regulated group included six mitochondrial genes, suggesting that a kind of mitochondrial stress is involved in the pathology of PQBP-1 Tg mice (Marubuchi *et al.* 2005). The down-regulated gene was neural tropomodulin. All these data were reported previously (Marubuchi *et al.* 2005). Interestingly, the list included a trophic factor, HDGF, which was increased to 2.301 fold. We performed northern blot analysis and confirmed that HDGF

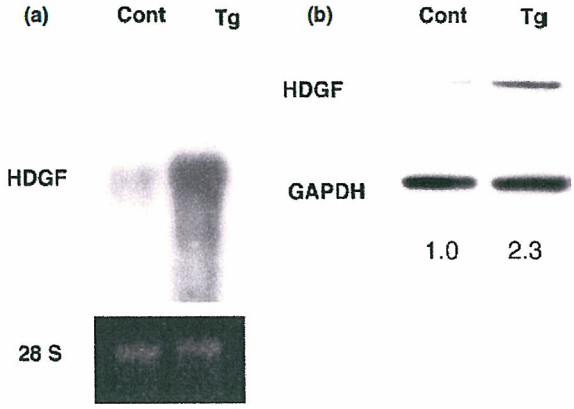

Fig. 1 HDGF mRNA and protein expression is increased in the spinal cord of PQBP-1 Tg mice. (a) Northern blot analysis confirmed up-regulation of HDGF mRNA in the spinal cord of PQBP-1 Tg mice at 12 months. Cont, age-matched littermates; Tg, PQBP-1 Tg mice; 28S, 28S ribosomal RNA. (b) Western blot analysis of the anterior horn of spinal cord from Tg mice (12 months old) and age-matched littermates (each $n = 3$). The expression ratios corrected with respect to glyceraldehyde-3-phosphate-dehydrogenase (GAPDH) are shown below the panels. HDGF protein expression was increased in the spinal cord of Tg mice.

mRNA was actually increased (Fig. 1a) HDGF was not increased at 2 months (Marubuchi *et al.* 2005).

To investigate the protein expression level of HDGF in Tg mice, we generated antibodies against human and rat C-terminal sequences. In parallel, we made recombinant mouse HDGF to test the specificity of these antibodies. HDGF was cleaved from GST-HDGF fusion protein by factor Xa, and purified with heparin column (Supplementary Fig. S1a). We generated specific antibodies against mouse and human HDGF C-terminal peptides (Fig. S1b), and confirmed by western blot that the 37-kDa band of HDGF was increased in the spinal cord of Tg mice (Fig. 1b).

The genes changed in the spinal cord of Tg mice include mitochondrial genes tRNA(Cys), tRNA(Glu), cytochrome C oxidase (CCO)1, CCO2, and Protein4, RNA polymerase I (Pol I) transcription-related factor [rRNA promoter-binding protein (Ribin)] (Kermekchiev and Ivanova 2001), heterogeneous nuclear ribonucleoproteins methyltransferase-like 2/protein arginine methyltransferase (Hrmtl2/PRMT) (Gary *et al.* 1996; Lin *et al.* 1996), a growth factor (HDGF) (Nakamura *et al.* 1994), receptor type Z protein tyrosine phosphatase (Krueger *et al.* 1990; Krueger and Saito 1992), MOR 6.5 (mouse genomic sequence relevant to ouabain resistance) (Zhou *et al.* 1993), and two unknown genes. We reported previously that PQBP-1 overexpression leads to a kind of mitochondrial stress and up-regulation mitochondrial genes (Marubuchi *et al.* 2005). The pathological relevance of the other genes will be reported elsewhere (Marubuchi *et al.*, unpublished observations).

HDGF protein is up-regulated in spinal motor neurons before degeneration

To identify the spinal cord cells that up-regulate HDGF protein, we performed immunohistochemical analysis of the lumbar spinal cords of PQBP1 Tg mice and littermates at 16 months (Fig. 2a). HDGF antibody (mC15-1) stained the largest neurons in the anterior horn that were not stained with GFAP antibody, i.e. motor neurons (Fig. 2a). Interestingly, nuclei of the anterior horn neurons were stained strongly in Tg mice but not in control mice (Fig. 2a). These data showed that HDGF expression in the nuclei of spinal motor neurons was remarkably up-regulated in PQBP-1 Tg mice. It is of note that anti-HDGF antibody stained some medium- or small-sized cells, which could be interneurons (Fig. 2a, thin arrows). HDGF was also expressed in the other neurons of the CNS including cortical neurons, as reported previously (Abouzied *et al.* 2004). However, no remarkable change in immunostaining was detected in neurons of PQBP-1 Tg mice other than spinal motor neurons (data not shown).

To understand the relevance of HDGF to amylotrophic lateral sclerosis (ALS), we asked whether the increased HDGF expression is observed in the motor neurons of mutant superoxide dismutase I (SOD1) mice (G93A). At 2 months, when the mutant SOD1 mice have not yet shown symptoms, HDGF was strongly stained in a part of the motor neuron nuclei, whereas staining in motor neurons was very weak in the age-matched control mice (Fig. 2b).

HDGF promotes neurite extension of motor neurons *in vitro*

HDGF is known to act as a trophic factor for dividing cells (Nakamura *et al.* 1989; Oliver and Al-Awqati 1998; Everett *et al.* 2000). Therefore, up-regulation of HDGF in spinal motor neurons of the mouse model of neurodegeneration prompted us to test whether HDGF acts as a trophic factor for motor neurons.

First, we observed its effect on neurite extension of spinal motor neurons. We synthesized recombinant mouse HDGF and added it to slices of lumbar spinal cord of E14 rat embryos cultured in medium with neither serum nor growth factors. As a control, mock solution, which was prepared from non-transformed *E. coli* cells exactly in the same manner as HDGF, was used. The comparison revealed that HDGF remarkably enhanced neurite extension (Fig. 3a). To distinguish neurites of motor neurons, we stained the slices with ChAT antibody. Extension of ChAT-positive neurites was also remarkably enhanced by HDGF (Fig. 3a). Quantitative analyses confirmed the effect of HDGF on neurite extension of spinal motor neurons (Fig. 3b). Most ChAT-positive neurons prepared from the anterior horn were considered to be motor neurons because E14 is the developmental stage at which motor neurons increase very rapidly and because we carefully separated the anterior horn from the

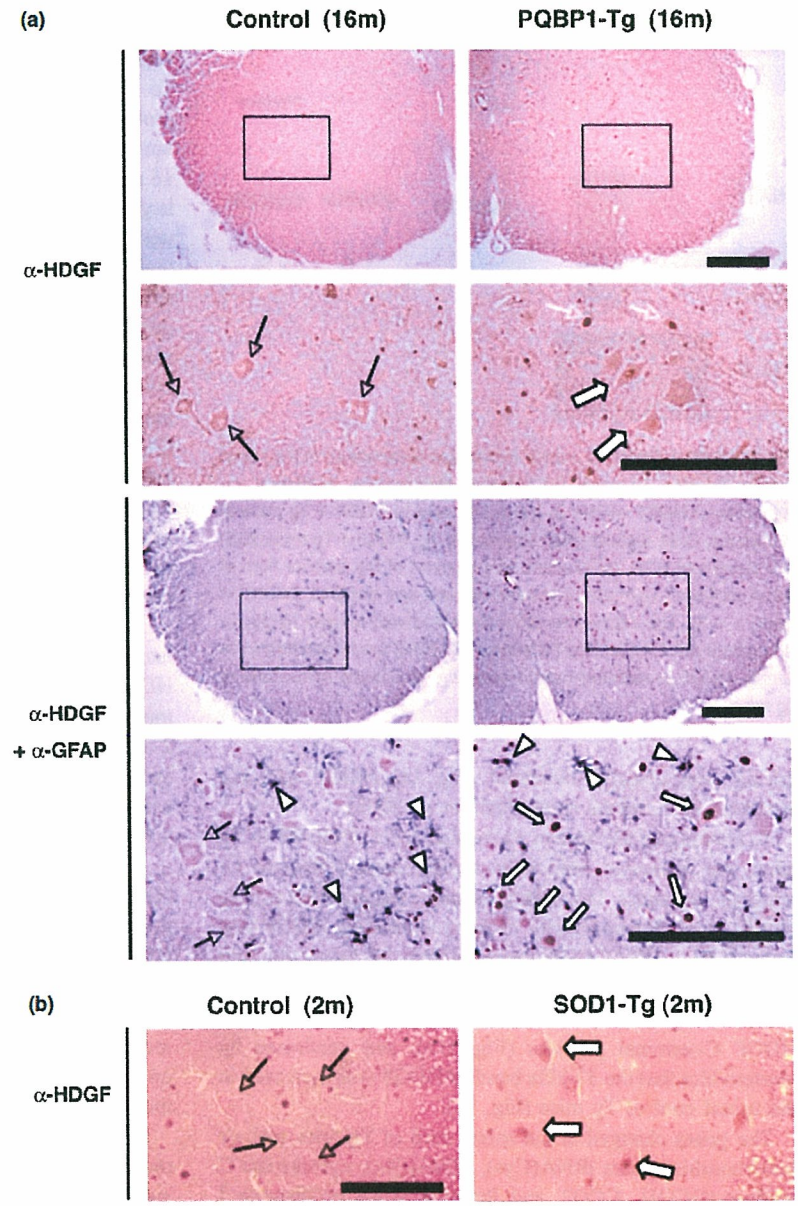

Fig. 2 HDGF is increased in spinal motor neurons of Tg mice. (a) Immunohistochemistry showing that HDGF protein was increased in spinal motor neurons of PQBP-1 Tg mice at 16 months. The upper panels show single staining with anti-HDGF antibody (mC15-1) and the lower panels show double staining with anti-HDGF (brown) and anti-GFAP antibody (blue). Higher magnifications (2nd and 4th rows) show that HDGF was increased in the nuclei of motor neurons (thick white arrows) and some other cells (thin white arrows) of Tg mice. On the other hand, the nuclei were not stained in most motor neurons of control mice (black arrows). GFAP staining (4th row) revealed that the large HDGF-positive cells were neurons. Glial cells (black) are indicated by white arrowheads. Scale bars 50 μm. (b) HDGF expression was increased in the motor neurons of mutant SOD mice (G93A). At 2 months when no symptoms were observed, HDGF was strongly stained in some of the motor neuron nuclei of mutant SOD mice (right panel, white arrows), whereas the nuclei of motor neurons were very weakly stained in the age-matched control mice (left panel, black arrows). Smaller cells other than motor neurons were stained by HDGF antibody in control mice. Scale bar 50 μm.

lateral horn under the microscope to prevent contamination by preganglionic autonomic neurons in the lateral horn.

We next compared the neurite-promoting activities of HDGF and other trophic factors, and found that the activity of HDGF was equivalent to that of ciliary neurotrophic factor (CNTF), BDNF, interleukin (IL)-6 and basic fibroblast growth factor (bFGF) (Fig. 3c). The trophic effect of HDGF was increased additively by any one of these trophic factors (data not shown), indicating that HDGF bound to a distinct receptor.

It is of note that a number of ChAT-positive neurons spread around the slice tissue in the presence of HDGF (Fig. 3a). This suggests enhanced migration by HDGF, although further investigations are necessary to confirm this assumption.

HDGF promotes survival of motor neurons *in vitro*

To test whether HDGF promotes survival of motor neurons in primary culture, spinal cord tissues of E14 rat embryos were dissected, mechanically dispersed, cultured for 7 days in serum-free medium with or without HDGF, and stained with ChAT antibody (Fig. 4a). As a control, we used the mock solution described above. Survival of the ChAT-positive neurons was clearly increased by addition of 3 or 30 ng/mL HDGF, and the effect of HDGF was almost equivalent to that of BDNF (Fig. 4a). Quantitative analyses

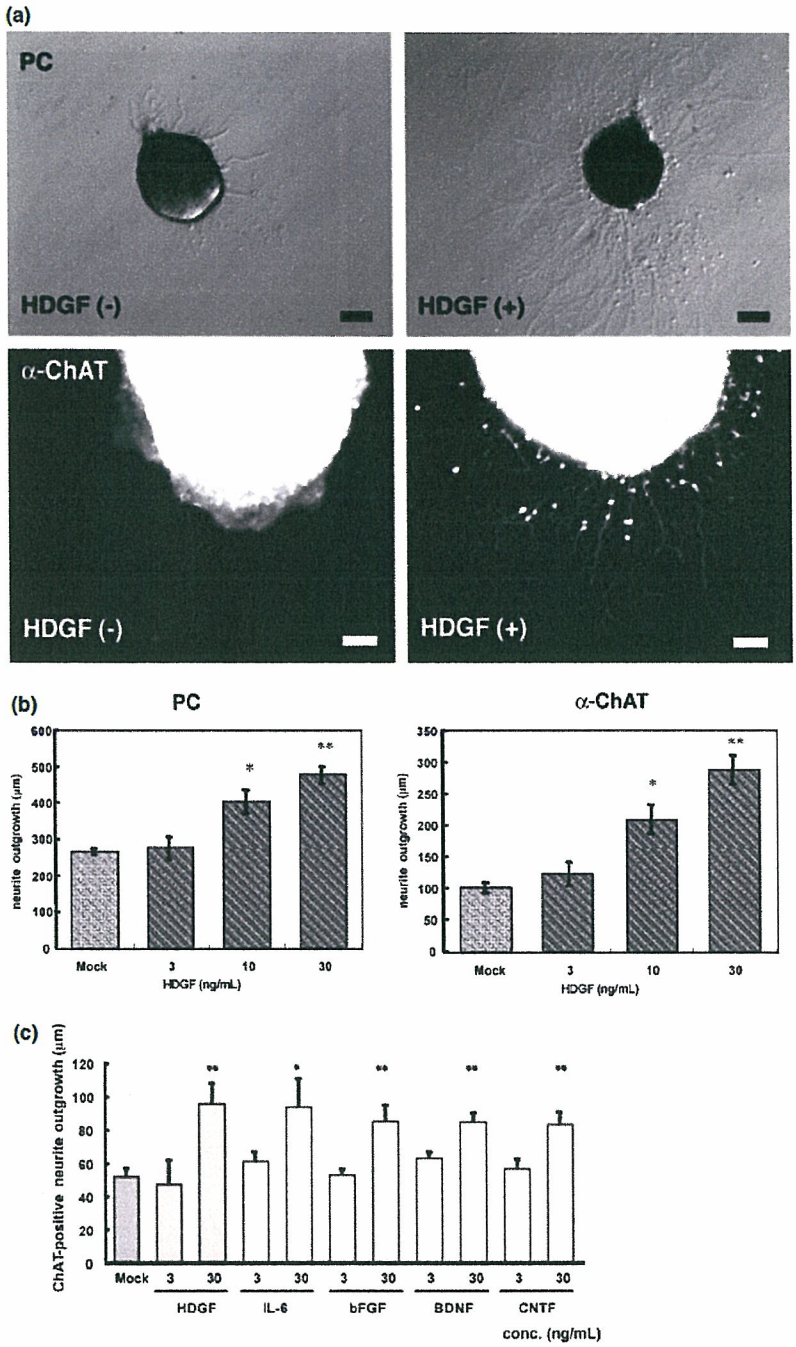

Fig. 3 HDGF promotes neurite extension of spinal motor neurons *in vitro*. (a) Recombinant mouse HDGF was added to slice cultures of rat embryonic spinal cord (E14). Phase-contrast images (PC) show that neurite extension was remarkably promoted 2 days after addition of HDGF (upper panels). HDGF also promoted neurite extension of ChAT-positive motor neurons (lower panels). Scale bars 10 μm. (b) Quantitative analysis by WinROOF (Mitani Corporation) confirmed dose-dependent neurite outgrowth in response to HDGF. Mock solution prepared from non-transformed *E. coli* cells was used as a control. Mean = SD, $^{*}p < 0.05$, $^{**}p < 0.01$ versus control (Dunnet test). (c) Comparison of the ChAT-positive neurite outgrowth between HDGF and other trophic factors. Mean = SD, $^{*}p < 0.05$, $^{**}p < 0.01$ versus mock control (Student's *t*-test).

of ChAT-positive motor neurons in 20 visual fields conformed that HDGF elongated survival of motor neurons (Fig. 4b). Together with the result of Fig. 3, these results strongly suggest that HDGF is a trophic factor for spinal motor neurons.

We also performed the neurite extension and neuron survival assays with spinal cords from E14 rat embryos of PQBP-1 Tg mice. Motor neurons from the transgene-positive embryos and those from negative embryos showed a similar response to HDGF in both assays (data not shown).

HDGF promotes survival of facial motor neurons *in vivo*

We examined the effect of HDGF on the survival of motor neurons in newborn rats after facial nerve section, which has been used to evaluate the effect of CNTF and BDNF on motor neurons (Sendtner *et al.* 1990, 1992). The proximal

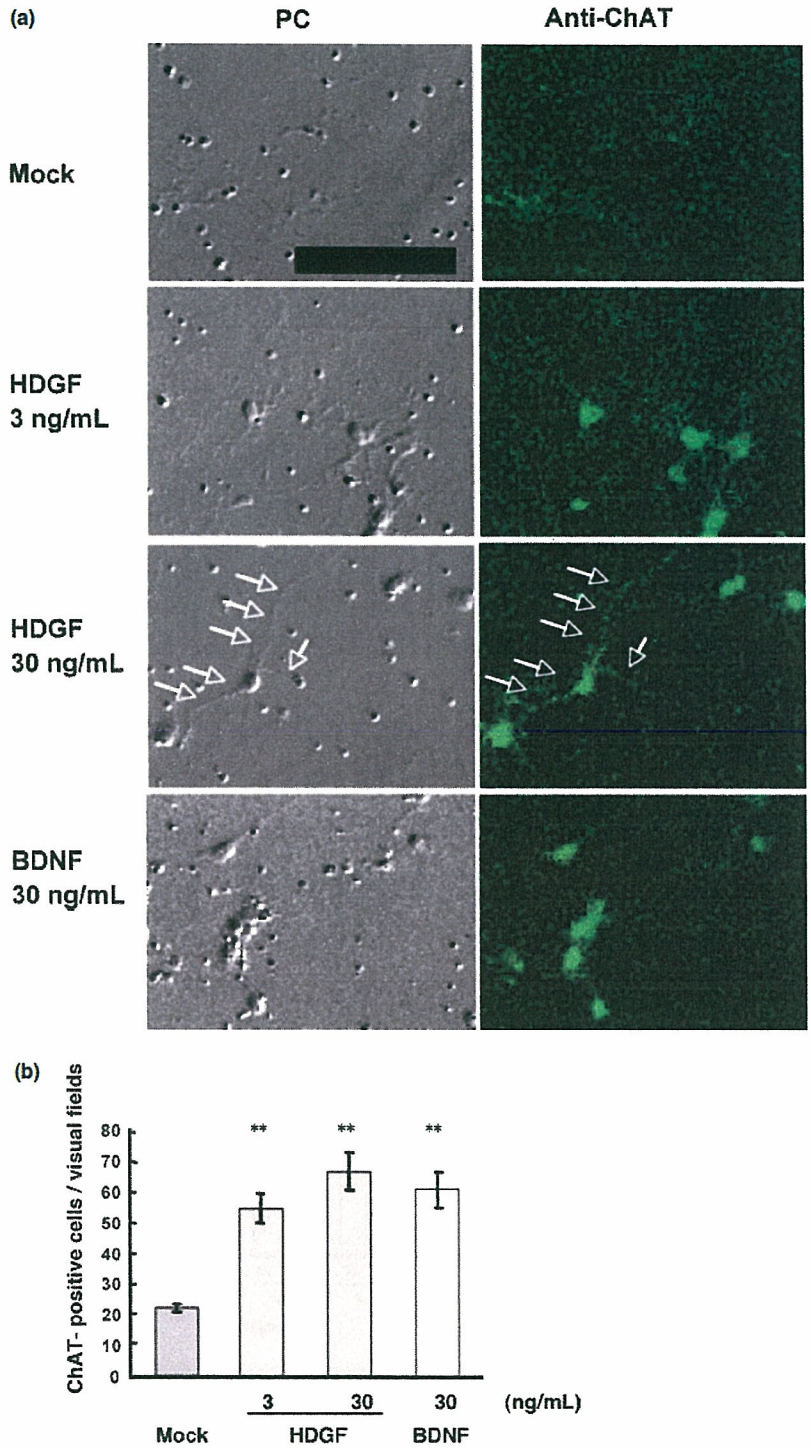

Fig. 4 HDGF promotes survival of spinal motor neurons *in vitro*. (a) Embryonic rat (E14) neurons form the anterior horn were mechanically dissociated and cultured in medium containing no serum or trophic factors. Seven days after addition of mock solution, HDGF or BDNF, survival of motor neurons was estimated by immunostaining with ChAT antibody. The number of ChAT-positive neurons was increased by addition of HDGF or BDNF. HDGF clearly promoted neurite outgrowth (white arrows). Scale bar 10 μm. (b) Quantitative analysis of survival of ChAT-positive neurons in 20 visual fields. Mean = SD $^{**}p < 0.01$ versus mock control (*t*-test).

nerve end after operation was treated with a piece of gel foam soaked with mock, HDGF or BDNF solution (each $n = 5$) and the survival of motor neurons in the facial nerve nucleus was analyzed morphologically after 7 days (Fig. 5). We made serial sections of 6 μm thickness from paraffin-embedded blocks of the brainstem, stained one every six sections with cresyl violet (Nissl staining), counted neurons in the facial nerve nucleus on injured and uninjured sides,

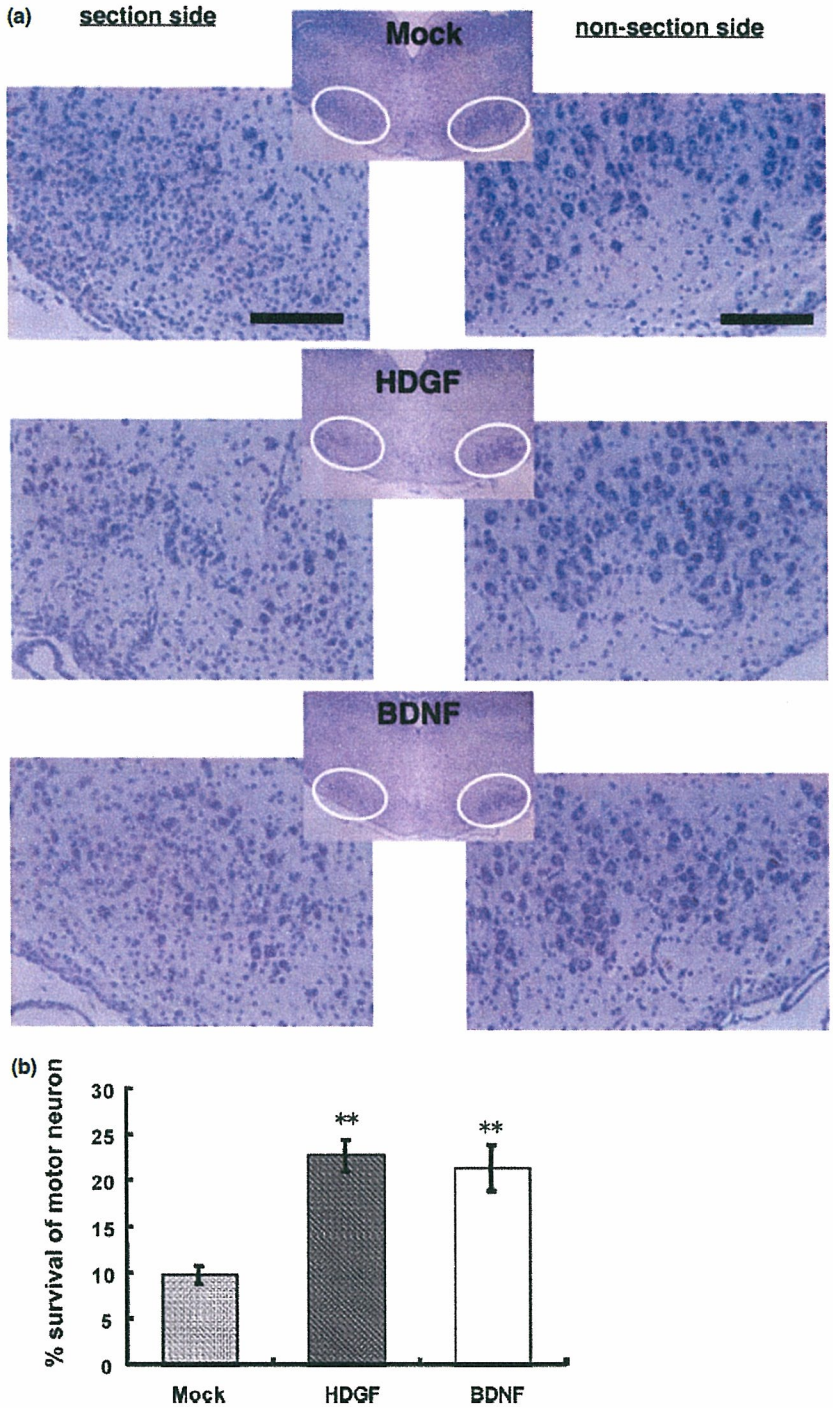

Fig. 5 HDGF promotes survival of facial motor neurons *in vivo*. (a) Representative pictures of the facial nuclei in mock-, HDGF- and BDNF-treated newborn rats (each $n = 5$). The slides were stained by cresyl violet to visualize rough endoplasmic reticulum (Nissl body) of neurons. High-power magnification of facial nuclei on sectioned and non-sectioned sides (left and right panels respectively) shows facial motor neurons distributed in the areas indicated by white circles in the low-power magnification images (central panels). Residual neurons became small and pyknotic. Proliferation of small reactive astrocytes (gliosis) was remarkable especially in mock-treated animals. Scale bars 10 μm. (b) The percentage survival was calculated as the ratio of the total number of facial motor neurons on sectioned side to that on non-sectioned side in each animal. A nucleolus was judged as a neuron. Mean = SD $^{**}p < 0.01$ versus mock control (*t*-test).

